

# Conduction mechanism in amorphous $\text{In}_2^{\text{III}}\text{X}_3^{\text{VI}}$ thin films

N. A. HEGAB, A. E. BEKHEET

*Physics Department, Faculty of Education, Ain Shams University, Cairo, Egypt*

Amorphous  $\text{In}_2^{\text{III}}\text{X}_3^{\text{VI}}$  films ( $X = \text{Te}$  or  $\text{Se}$ ) are obtained by vacuum thermal evaporation of bulk materials on glass substrates. The current - voltage characteristics in the temperature range 298–378 K and in the thickness range 212–652 nm exhibited a transition from an ohmic region in the lower field followed by non-ohmic region in the high field region, which has been explained by the anomalous Poole-Frenkel effect. The temperature dependence of current in the ohmic region is of thermally activated process. The variation of dielectric constant with temperature is investigated for the two compounds.

© 2001 Kluwer Academic Publishers

## 1. Introduction

$\text{In}_2\text{Te}_3$  and  $\text{In}_2\text{Se}_3$  are III–VI semiconducting compounds with very interesting electrical and optical properties [1–7]. These compounds are useful for many applications such as switching effect which was reported before [8, 9]. Since a high speed switching and memory effect of an amorphous semiconductor were reported [10, 11], its properties have been studied very actively. There have been several discussions on the mechanism of high speed switching and of electric conduction in amorphous materials.

The study of the pre-switching current voltage characteristics is necessary to identify the electrical conduction mechanism occurring in chalcogenide glass switches. The space charge limited current [12], hopping conduction [13], small polaron conduction [14] and the Poole-Frenkel conduction [15] are the possible conduction mechanisms.

In this paper the voltage and temperature dependence of current in  $\text{In}_2\text{Te}_3$  and  $\text{In}_2\text{Se}_3$  films, produced by vacuum deposition, were studied to discuss the possible conduction mechanism of charge transport.

## 2. Experimental

Two compounds of type  $\text{In}_2\text{Te}_3$  and  $\text{In}_2\text{Se}_3$  were prepared in bulk form as mentioned previously [7, 16]. Films with different thicknesses of  $\text{In}_2\text{Te}_3$  and  $\text{In}_2\text{Se}_3$  were obtained by thermal evaporation of the bulk samples, onto cleaned glass substrates provided with Al electrodes as lower and top electrodes for sandwich configuration of dimension 2 mm × 2 mm (Fig. 1). The substrate temperature was held below 50°C during deposition process. The film thickness was estimated during deposition by Edwards FTM5 thickness monitor, subsequently it was measured after deposition by multiple beam interferometry. X-ray diffractometer of the type Philips (PM 8203) was used to investigate the structure of the obtained samples in bulk and thin film forms. The current-voltage (I–V) characteristics were measured throughout the thickness range 212–654 nm

and within the temperature range 298–378 K, below the transition temperatures, which has been reported previously [7, 17], using electrometer (Keithley type E616A) for the potential drop measurements and a microdigit multimeter (TE 924) for the current measurements. The temperature of the sample was monitored using a chromel-alumel thermocouple.

## 3. Results and discussion

X-ray diffraction patterns carried out for powder and thin film forms are given in Fig. 2a and b for  $\text{In}_2\text{Te}_3$  and  $\text{In}_2\text{Se}_3$  which indicate the amorphous nature of  $\text{In}_2\text{Te}_3$  in both powder and thin film forms, However  $\text{In}_2\text{Se}_3$  in bulk form has polycrystalline nature of  $\alpha$ -phase, and its thin film form has amorphous nature.

### 3.1. I–V characteristics

Fig. 3a and b presents the current-voltage (I–V) characteristics for  $\text{In}_2\text{Te}_3$  and  $\text{In}_2\text{Se}_3$  thin films at different temperatures in the range 298 to 378 K. It is clear that the relations are linear for lower voltages indicating ohmic conduction, which is controlled by electron hopping, and become non-linear at higher voltages. It is also observed from Fig. 3 that the linear regions extend to higher values of the applied field with increasing temperature. Similar results have been obtained previously for other amorphous semiconductor materials [18]. The I–V characteristics exhibited an ohmic region at low applied voltage with low field followed by a transition to supra linear at higher voltage with high field up to the breakdown voltage value. Fig. 4a and b shows the I–V characteristics at room temperature for the two compound with different thicknesses which gives the same behavior. Several factors must be examined to analyze this behavior, such as the effect of sample thickness and electrode materials on the conductivity. It was found that the conductivity is independent of these factors [16, 17], which suggest that space charge limited conduction and Schottky emission

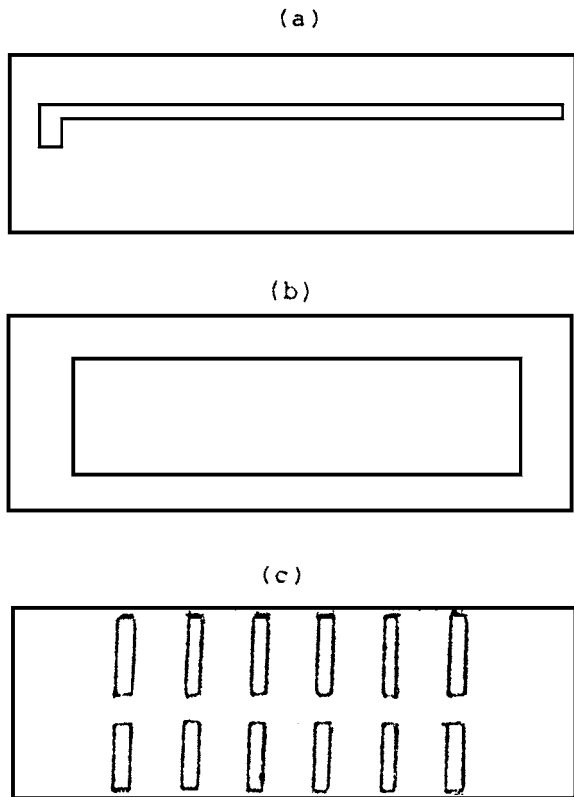


Figure 1 Deposition masks for sandwich structure: (a) mask for bottom electrode (2 mm width), (b) mask for semiconductor material, (c) mask for top electrode (2 mm width).

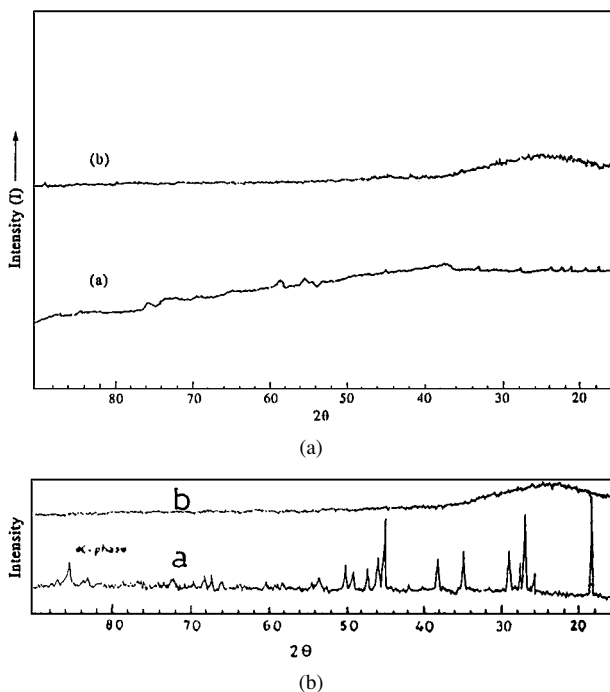


Figure 2 (a) X-ray diffraction pattern of  $\text{In}_2\text{Te}_3$  in curve (a) bulk form and curve (b) thin film form. (b) X-ray diffraction pattern of  $\text{In}_2\text{Se}_3$  in curve (a) bulk form and curve (b) thin film form.

do not determine the conduction mechanism and consequently the field dependence was a property of the bulk material.

Fig. 5a and b shows the plot of  $I$  (in logarithmic scale) vs  $E^{1/2}$  for the data of Fig. 3a and b. It is clear from the

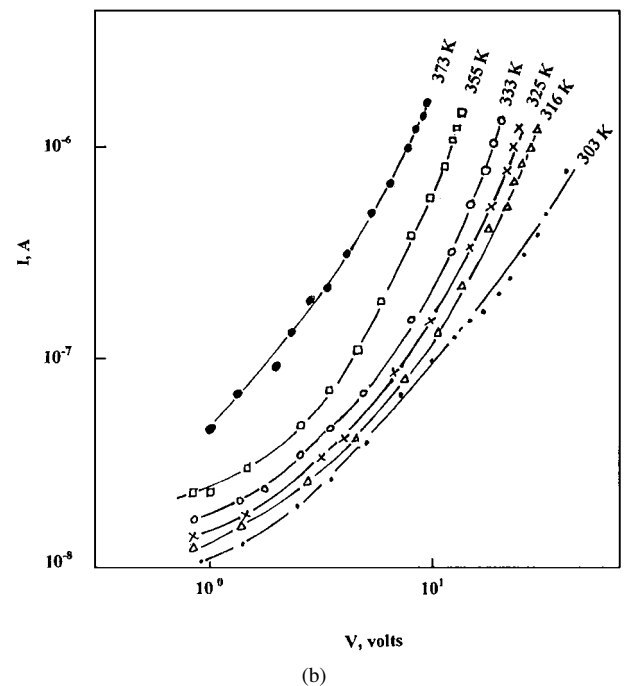
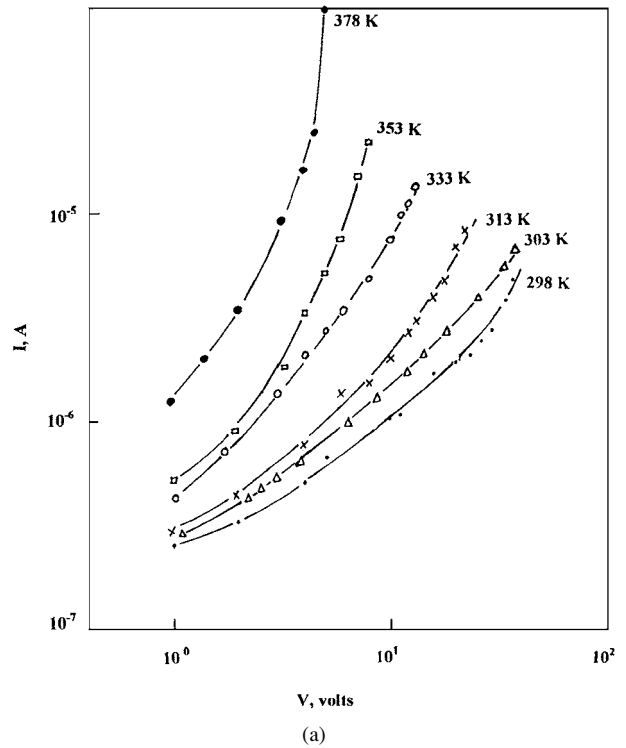


Figure 3 (a) Current-voltage characteristics at various temperatures for  $\text{In}_2\text{Te}_3$  film of thickness 592 nm. (b) Current-voltage characteristics at various temperatures for  $\text{In}_2\text{Se}_3$  film of thickness 532 nm.

figure that, there is a dependence of type  $I \propto E^{1/2}$  for  $\text{In}_2\text{Te}_3$  and  $\text{In}_2\text{Se}_3$  films over at least two order of magnitude of current. The linear portion of the graphs in the non ohmic region has been taken as evidence of either the Schottky [19], or Poole-Frenkel [20] effect as an operative conduction mechanism. However the temperature dependence of measurements at various fixed voltages suggest the Poole-Frenkel effect to be operative. Moreover the different parameters estimated from graphs found to lie in an acceptable range only when the Poole-Frenkel effect is assumed to be operative.

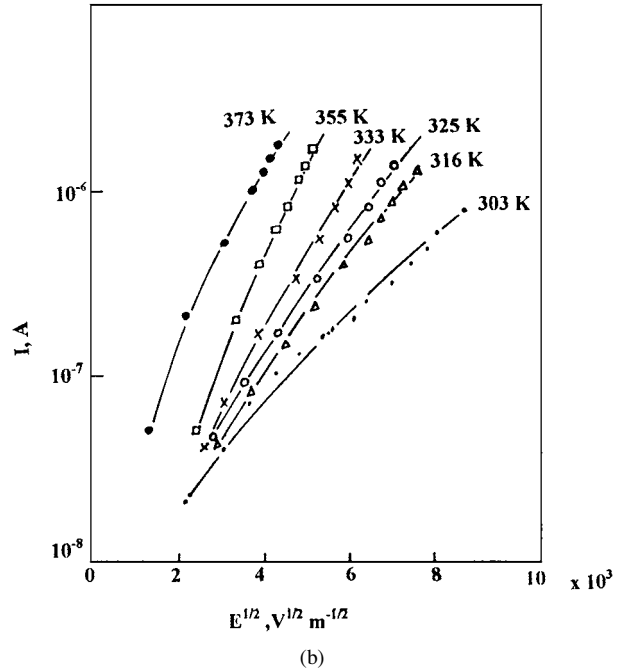
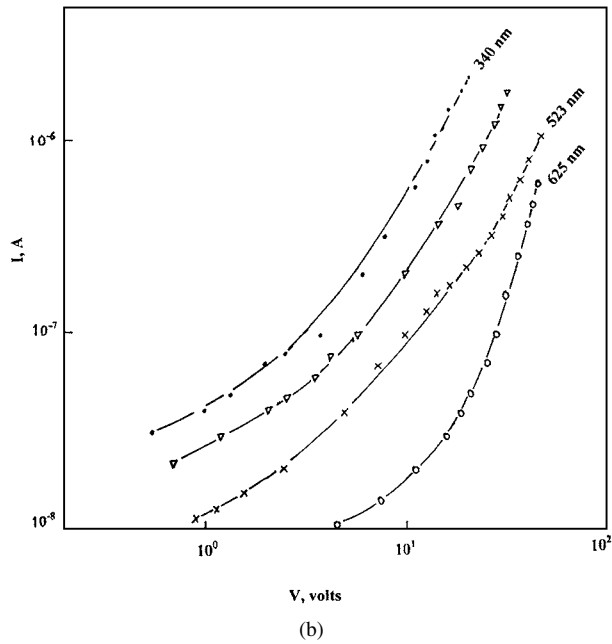
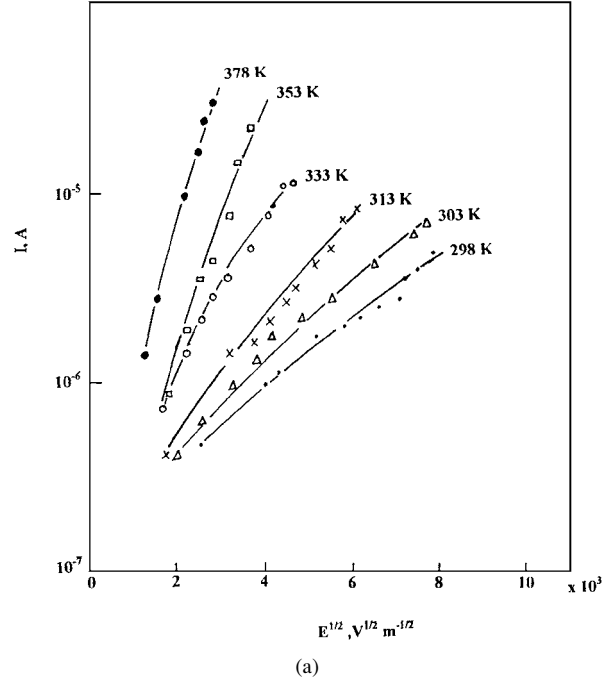
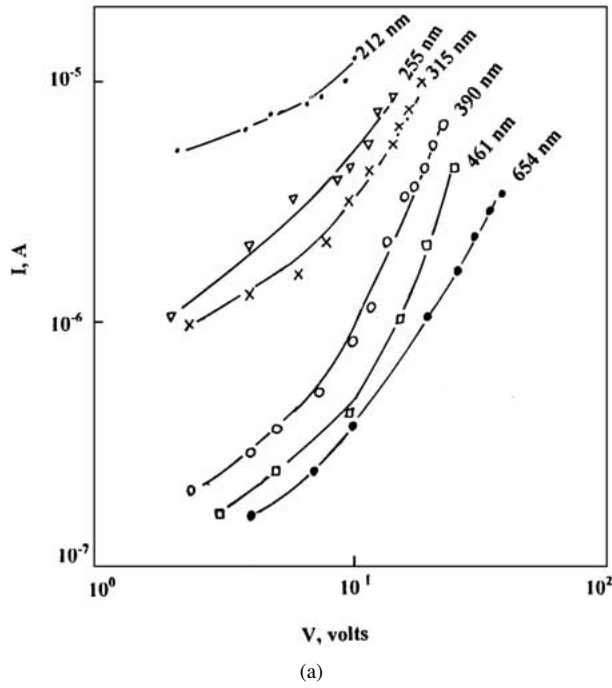


Figure 4 (a) Room temperature current-voltage characteristics for  $\text{In}_2\text{Te}_3$  films of different thicknesses. (b) Room temperature current-voltage characteristics for  $\text{In}_2\text{Se}_3$  films of different thicknesses.

Figure 5 (a)  $I$  (in logarithmic scale) vs  $E^{1/2}$  plots for the  $\text{In}_2\text{Te}_3$  film at different temperature. (b)  $I$  (in logarithmic scale) vs  $E^{1/2}$  plots for the  $\text{In}_2\text{Se}_3$  film at different temperature.

According to the Poole-Frenkel effect [20], the electric field interacts with the Coulombic potential barrier of a donor center or trap and the height of barrier is lowered. In the presence of an electric field ( $E$ ), the electrons are thermally emitted from the randomly distributed traps to the conduction band by the lowering of the Coulombic potential barrier by the external electric field. The current density ( $J$ ) for thin film containing shallow traps is given by:

$$J = J_0 \exp(\beta_{\text{PF}} E^{1/2} / kT) \quad (1)$$

Where  $J_0$  is the low field current density,  $E$  is the applied electric field,  $k$  is the Boltzmann constant,  $T$  is

the absolute temperature and  $\beta_{\text{PF}}$  is the Poole-Frenkel field lowering coefficient which is given by:

$$\beta_{\text{PF}} = (e^3 / \Pi \epsilon \epsilon_0)^{1/2} \quad (2)$$

where  $e$  is the electronic charge,  $\epsilon_0$  is the permittivity of the free space, and  $\epsilon$  is the dielectric constant of material.

Now,  $\beta_{\text{PF}}$  can be calculated theoretically according to Equation 2 for which the dielectric constant  $\epsilon$  of the sample under investigation has been determined. The slope of the linear part in the non-ohmic region of curves 5 (a) and (b) gives the values of  $\beta_{\text{PF}}$  and its

TABLE I Variation of  $\beta$  and  $\epsilon$  with temperature for  $\text{In}_2\text{Te}_3$  film of thickness 592 nm

Temperature K	Poole-Frenkel Model				Jonscher Model			
	Log $I$ vs $E^{1/2}$		Log $IE^{-1}$ vs $E^{1/2}$		Log $IE^{1/2}$ vs $E^{1/2}$		Log $IE^{-1/2}$ vs $E^{1/2}$	
	$\beta/10^{-5}$ $\text{eVm}^{1/2} \text{V}^{-1/2}$	Dielectric constant $\epsilon$	$\beta/10^{-5}$ $\text{eVm}^{1/2} \text{V}^{-1/2}$	Dielectric constant $\epsilon$	$\beta/10^{-5}$ $\text{eVm}^{1/2} \text{V}^{-1/2}$	Dielectric constant $\epsilon$	$\beta/10^{-5}$ $\text{eVm}^{1/2} \text{V}^{-1/2}$	Dielectric constant $\epsilon$
298	1.797	17.793	1.602	22.295	1.935	15.371	1.819	17.058
303	1.877	16.308	1.867	16.4697	1.918	15.609	1.964	14.890
313	2.033	13.932	1.807	17.633	2.033	13.931	2.032	13.944
333	2.884	6.924	2.395	10.039	3.145	5.818	2.479	9.366
353	3.389	5.011	3.057	6.162	3.73	4.138	3.056	6.161
378	3.629	4.37	4.078	3.463	3.89	3.80	3.891	3.802

TABLE II Variation of  $\beta$  and  $\epsilon$  with temperature for  $\text{In}_2\text{Se}_3$  film of thickness 532 nm

Temperature K	Poole-Frenkel Model				Jonscher Model			
	Log $I$ vs $E^{1/2}$		Log $IE^{-1}$ vs $E^{1/2}$		Log $IE^{1/2}$ vs $E^{1/2}$		Log $IE^{-1/2}$ vs $E^{1/2}$	
	$\beta/10^{-5}$ $\text{eVm}^{1/2} \text{V}^{-1/2}$	Dielectric constant $\epsilon$	$\beta/10^{-5}$ $\text{eVm}^{1/2} \text{V}^{-1/2}$	Dielectric constant $\epsilon$	$\beta/10^{-5}$ $\text{eVm}^{1/2} \text{V}^{-1/2}$	Dielectric constant $\epsilon$	$\beta/10^{-5}$ $\text{eVm}^{1/2} \text{V}^{-1/2}$	Dielectric constant $\epsilon$
303	1.964	14.895	2.014	14.165	2.019	14.091	2.014	14.165
316	2.366	10.287	2.118	12.835	2.052	13.669	2.075	13.37
325	2.814	7.123	2.801	7.341	2.604	8.494	2.232	11.555
333	2.843	7.108	2.895	6.685	2.665	8.104	2.472	9.424
355	3.335	5.175	3.309	5.256	3.074	6.093	3.063	6.134
373	3.413	4.94	3.494	4.718	3.230	5.519	3.255	5.431

values are listed in Tables I and II for the two systems under investigation. The experimental value of  $\beta_{\text{PF}}$  at room temperature obtained by the aid of Equation 2 is about  $2.033 \times 10^{-5} \text{ eVm}^{1/2}\text{V}^{-1/2}$  for  $\text{In}_2\text{Te}_3$  film. Using the estimated value of  $\epsilon = 10.46$  obtained before [21], the calculated value of  $\beta_{\text{PF}}$  using Equation 2 is  $2.346 \times 10^{-5} \text{ eVm}^{1/2}\text{V}^{-1/2}$  and the Schottky coefficient  $\beta_{\text{S}} = 1/2\beta_{\text{PF}} = 1.173 \times 10^{-5} \text{ eVm}^{1/2}\text{V}^{-1/2}$ . Similarly, the experimental value of  $\beta_{\text{PF}}$  at room temperature for  $\text{In}_2\text{Se}_3$  films is about  $2.366 \times 10^{-5} \text{ eVm}^{1/2}\text{V}^{-1/2}$ . Using the estimated value of  $\epsilon = 9.9$  obtained before [7] the calculated value of  $\beta_{\text{PF}} = 2.412 \times 10^{-5} \text{ eVm}^{1/2}\text{V}^{-1/2}$  and the Schottky coefficient  $\beta_{\text{S}} = 1/2\beta_{\text{PF}} = 1.206 \times 10^{-5} \text{ eVm}^{1/2}\text{V}^{-1/2}$ . These calculations suggested that the experimental values of  $\beta_{\text{PF}}$  is in agreement with the Poole-Frenkel mechanism rather than the Schottky mechanism. However this agreement between the experimental and theoretical values of  $\beta_{\text{PF}}$  cannot be taken for suggesting the conduction mechanism which will be operated. Values of  $\beta_{\text{PF}}$  at different temperatures obtained experimentally are listed in Tables I and II. It is clear from Tables I and II that the experimental values of  $\beta_{\text{PF}}$  for  $\text{In}_2\text{Te}_3$  and  $\text{In}_2\text{Se}_3$  thin films have an apparent dependence on temperature through the investigated range of temperature.

The variation of  $I$  (in logarithmic scale) vs  $E^{1/2}$  at room temperature for the two amorphous  $\text{In}_2\text{Te}_3$  and  $\text{In}_2\text{Se}_3$  films is shown in Fig. 6. It is clear from the figure that for a constant value of the applied voltage, a decrease in electrical conductivity for  $\text{In}_2\text{Se}_3$  than for  $\text{In}_2\text{Te}_3$  is observed. The presence of a high concentration of localized states in the band structure is responsible for the larger value electrical conductivity the case of the  $\text{In}_2\text{Te}_3$  amorphous films [22].

Using the values of  $\beta_{\text{PF}}$ , listed in Tables I and II values of the dielectric constant  $\epsilon$  at different temperatures

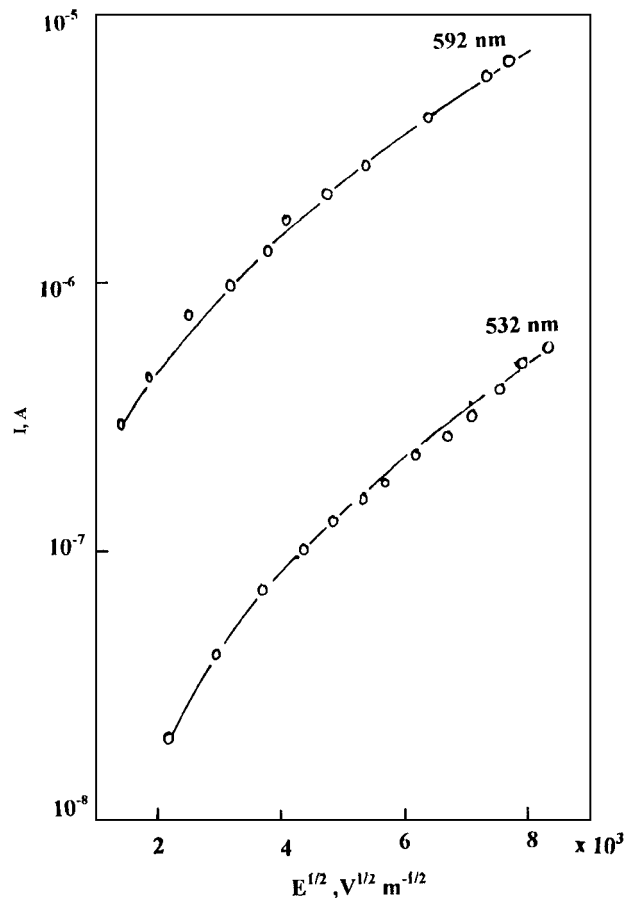


Figure 6  $I$  (in logarithmic scale) vs  $E^{1/2}$  plots for the  $\text{In}_2\text{Te}_3$  and  $\text{In}_2\text{Se}_3$  films at room temperature.

were estimated according to Equation 2 and are listed in the tables. It is clear from the tables that values of  $\epsilon$ , at any given temperature, for  $\text{In}_2\text{Te}_3$  is higher than their values for  $\text{In}_2\text{Se}_3$  films. Since the bond energy of Se-Se

bond is higher than its value for Te-Te bond [23]. Also since the electronegativity of Se is stronger than Te, the In-Se bond is stronger than In-Te bond in the two systems [21, 24]. So  $\text{In}_2\text{Te}_3$  can respond to the electric field much easier than  $\text{In}_2\text{Se}_3$ .

### 3.2. I-T characteristics

The temperature dependence of the current was studied for the as-deposited  $\text{In}_2\text{Te}_3$  and  $\text{In}_2\text{Se}_3$  films for different fixed applied voltages in the temperature range 298–378 K, taking in consideration the importance of these characteristics for the proper choice of charge transfer model. The obtained curves ( $I$  (in logarithmic scale) versus  $1/T$ ) for the two systems under test are shown in Fig. 7a and b. It is clear from the figure that all the obtained relations are straight lines indicating that the conduction in these films takes place through an activated process having a single activation energy in the considered temperature range.

The activation energy  $\Delta E_\sigma$  was calculated for the investigated samples from the slopes of the straight lines of Fig. 7 and using the following equation:

$$I = I_0 \exp -\Delta E_\sigma / kT \quad (3)$$

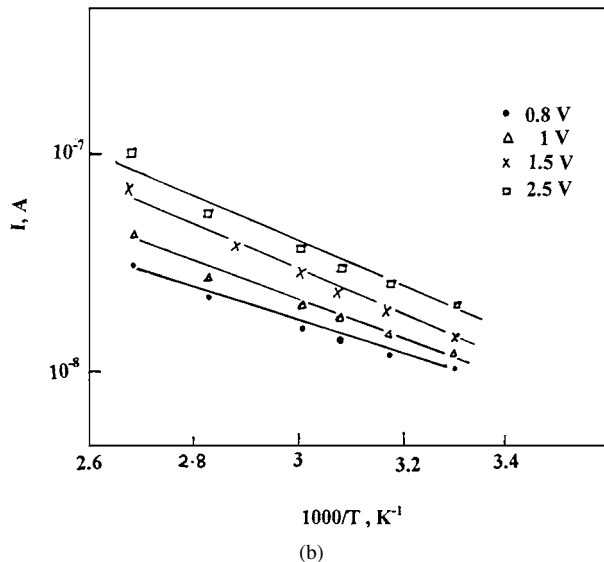
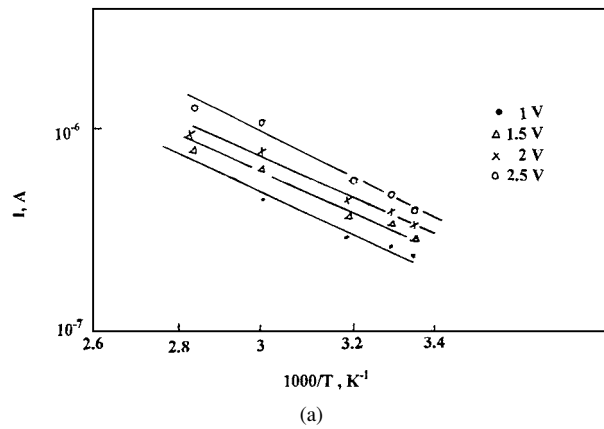


Figure 7 (a)  $I$  (in logarithmic scale) vs  $1000/T$  for  $\text{In}_2\text{Te}_3$  film at different fixed applied voltage. (b)  $I$  (in logarithmic scale) vs  $1000/T$  for  $\text{In}_2\text{Se}_3$  film at different fixed applied voltage.

TABLE III Activation energy of  $\text{In}_2\text{Te}_3$  film of thickness 592 nm and  $\text{In}_2\text{Se}_3$  film of thickness 532 nm at various applied bias

$\text{In}_2\text{Te}_3$		$\text{In}_2\text{Se}_3$	
Applied bias (V)	Activation Energy ( $\Delta E_\sigma$ ) eV	Applied bias (V)	Activation Energy ( $\Delta E_\sigma$ ) eV
1	0.56	0.8	0.395
1.5	0.52	1	0.416
2	0.54	1.5	0.48
2.5	0.54	2.5	0.395

where  $I_0$  is the current extrapolated to  $1/T = 0$ . The calculated values of  $\Delta E_\sigma$  are given in Table III which are in agreement with that obtained before [16, 17]. The slopes of the curves do not vary appreciably with the applied voltage (See  $\Delta E_\sigma$  values). It was found that the electrical conductivity of  $\text{In}_2\text{Te}_3$  is higher than

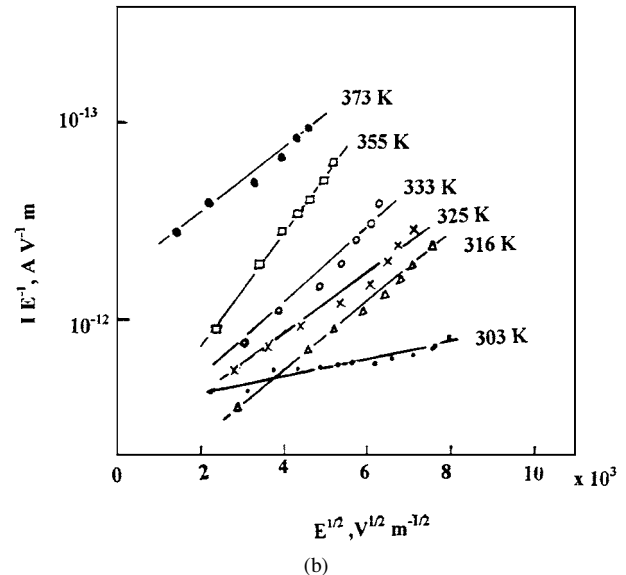
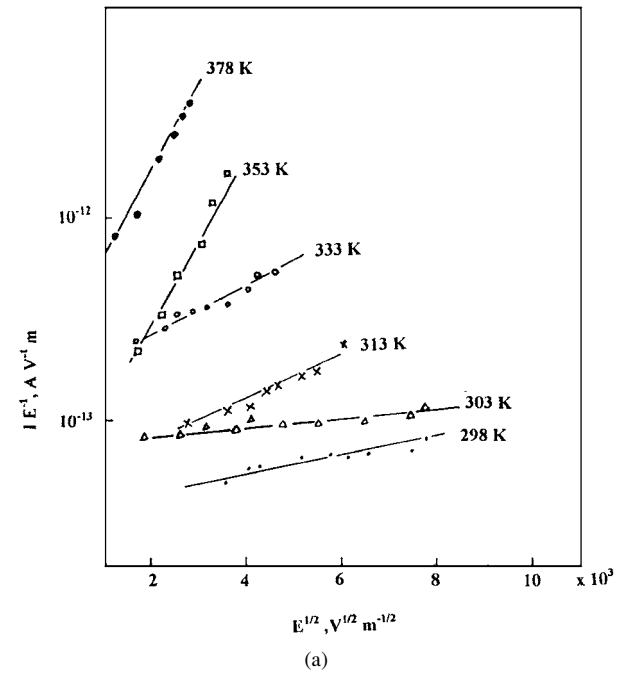


Figure 8 (a)  $I E^{-1}$  (in logarithmic scale) vs  $E^{1/2}$  for the  $\text{In}_2\text{Te}_3$  film at different temperature. (b)  $I E^{-1}$  (in logarithmic scale) vs  $E^{1/2}$  for the  $\text{In}_2\text{Se}_3$  film at different temperature.

that of  $\text{In}_2\text{Se}_3$ . This result is attributed to the nature of chemical bonding in the two systems. Since Te-Te and Se-Se bond energies [23] are 193 and 223 kJ/mol, it is reasonable that Se-In bond energy is higher than Te-In bond energy and so the conductivity of  $\text{In}_2\text{Te}_3$  is higher than that of  $\text{In}_2\text{Se}_3$ . This is confirmed by the values of electronegativity difference for the elements Se, In and Te, In [21, 24]. The larger the difference, the more likely bond will form. The activation energy of  $\text{In}_2\text{Se}_3$  films is less than expected in the case of most semiconductor materials (half of the optical energy gap (1.37 eV)) [7]. This low value of  $\Delta E_\sigma$  was explained before [25] by a proposed model for the band structure of  $\text{In}_2\text{Se}_3$ . According to this model, an energy band in

the energy gap originates from the six-co-ordinated In atoms. This model predicts that  $\Delta E_\sigma$  is  $\frac{1}{4}E_g^{\text{opt}}$ , which agrees with the obtained results.

### 3.3. Poole-Frenkel mechanism and its modification

In order to specify the dominant mechanism for conduction in the high field region, data of Fig. 5a and b are plotted in accordance with high electric field theory to establish the Poole-Frenkel effect if it dominant. Fig. 8a and b show linear plots of  $I E^{-1}$  (in a logarithmic scale) vs  $E^{1/2}$  as required by the Poole-Frenkel equation [20]. The derived value of  $\beta_{\text{PF}}$  and  $\epsilon$  are given in Tables I and II. For example the slope of the straight lines gives  $\beta_{\text{PF}}$  equal to  $1.771 \times 10^{-5} \text{ eVm}^{1/2}\text{V}^{-1/2}$  for  $\text{In}_2\text{Se}_3$  which yield a dielectric constant  $\epsilon = 18.357$  which is much higher than the theoretical value. It is observed that the field lowering coefficient  $\beta_{\text{PF}}$  increases with increasing temperature through the investigated range (298–378 K).

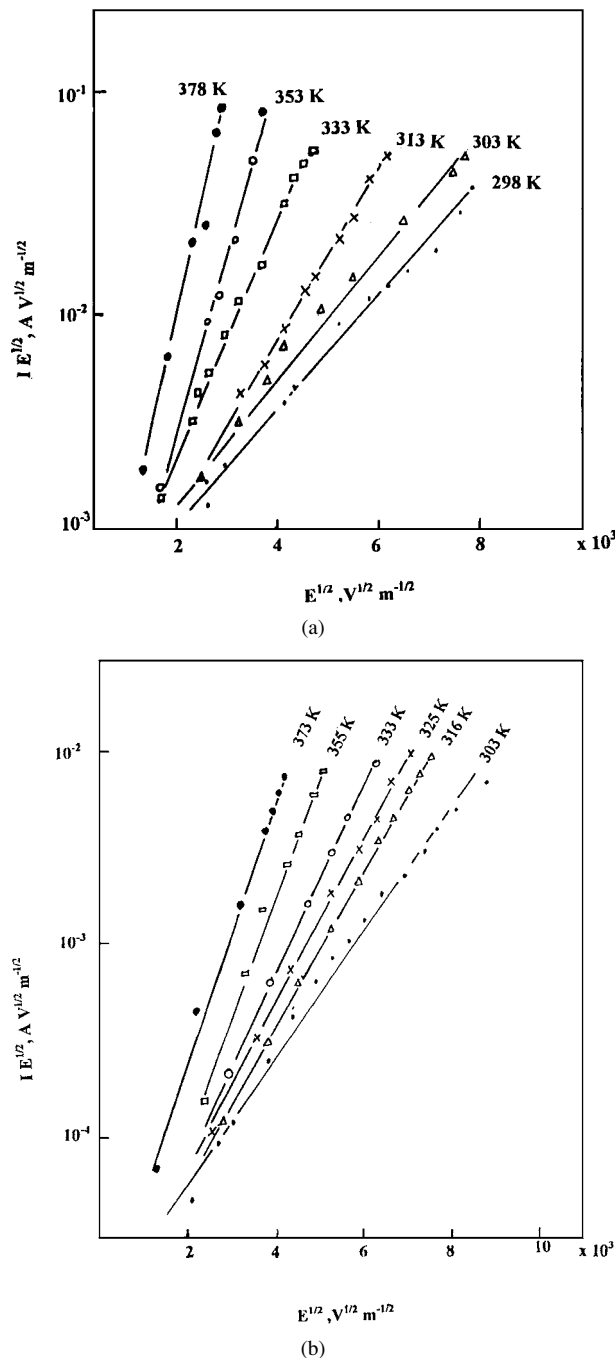


Figure 9 (a)  $I E^{1/2}$  (in logarithmic scale) vs  $E^{1/2}$  for the  $\text{In}_2\text{Te}_3$  film at different temperature. (b)  $I E^{1/2}$  (in logarithmic scale) vs  $E^{1/2}$  for the  $\text{In}_2\text{Se}_3$  film at different temperature.

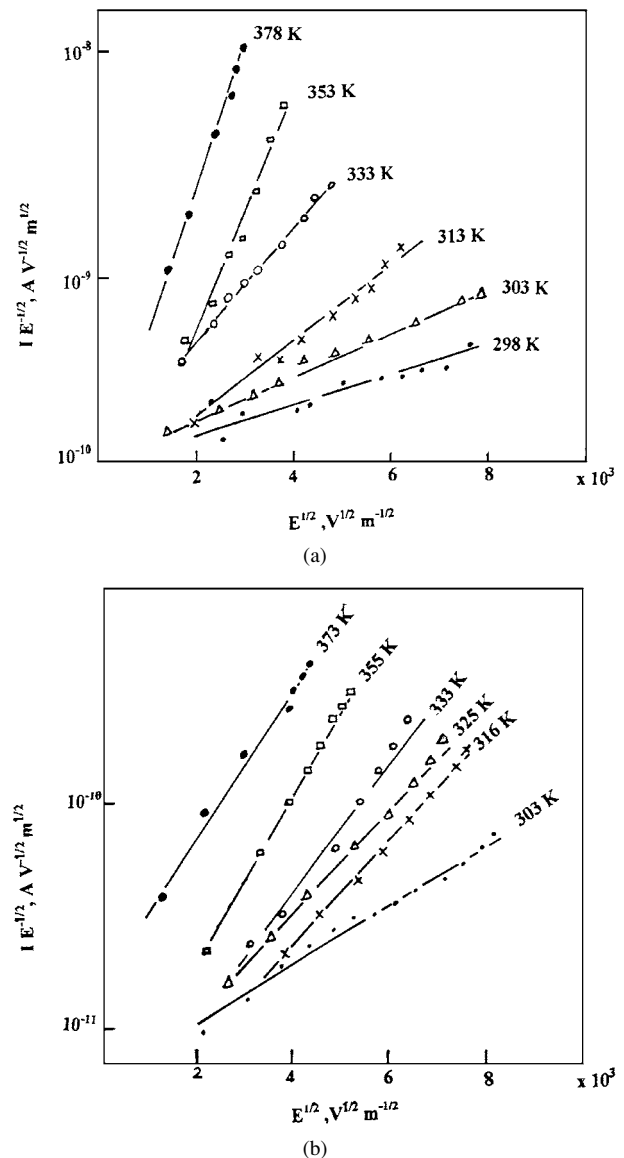


Figure 10 (a)  $I E^{-1/2}$  (in logarithmic scale) vs  $E^{1/2}$  for the  $\text{In}_2\text{Te}_3$  film at different temperature. (b)  $I E^{-1/2}$  (in logarithmic scale) vs  $E^{1/2}$  for the  $\text{In}_2\text{Te}_3$  film at different temperature.

Based on the Jonscher's model [26] (which takes account of the emission of electrons from sites in one particular direction in space with respect to the applied field) the data given in Fig. 3a and b for  $\text{In}_2\text{Te}_3$  and  $\text{In}_2\text{Se}_3$  films can be analyzed. Accordingly, plots of  $\log IE^{1/2}$  vs  $E^{1/2}$  characteristics can be obtained and illustrated in Fig. 9a and b for the two systems under investigation. The obtained values of  $\beta$  and  $\varepsilon$  are listed in Tables I and II. Fitting the room temperature data to the Jonscher model is an indication that a modified Poole-Frenkel process is operating.

Fig. 10a and b show the  $IE^{-1/2}$  (in a logarithmic scale) vs  $E^{1/2}$  characteristics for conduction model in which carrier motion are assumed to travel for a constant period of time before being trapped. The deduced values of  $\beta$  and  $\varepsilon$  are also given in Tables I and II.

Tables I and II show a large change in  $\beta_{\text{PF}}$  and  $\varepsilon$  for the tested systems on increasing temperature through the investigated range (298–378 K). Both the normal Poole-Frenkel and Jonscher models are able to explain this change.

#### 4. Conclusion

In the previous sections, we analyzed the electrical conduction in thin  $\text{In}_2\text{Te}_3$  and  $\text{In}_2\text{Se}_3$  films. The I–V characteristics of these films were obtained in the temperature range 298–378 K and thickness range 212–654 nm. These characteristics exhibited a transition from an ohmic region at low applied voltage to a non ohmic region at higher voltage arises from lowering of the potential barriers by a high electric field.

The dependence of ohmic current on temperature corresponds to a thermally activated process. The values of activation energy as well as the dielectric constant for  $\text{In}_2\text{Te}_3$  and  $\text{In}_2\text{Se}_3$  films were investigated.

#### References

1. S. A. HUSSEIN and A. T. NAGAT, *Phys. Stat. Soli. A* **114** (1989) K 205.
2. A. A. ZAHAB, M. ABD-LEFDIL and M. CADENE, *ibid.* **115** (1989) 491.
3. *Idem.*, *ibid.* **117** (1990) K103.
4. S. SEN and D. N. BOSE, *Solid State Commun* **50** (1984) 39.
5. C. JULIEN, M. EDDRIEF, K. KAMBAS and M. BALKANSKI, *Thin Solid Films* **137** (1986) 27.
6. K. KAMBAS and J. SPYRIDELIS, *Mat. Res. Bull.* **13** (1978) 653.
7. H. T. EL-SHAIR and A. E. BEKHEET, *J. Phys. D. Appl. Phys.* **25** (1992) 1122.
8. M. A. AFIFI, H. H. LABIB, N. A. HEGAB, M. FADEL and A. E. BEKHEET, *Indian Pure & Appl. Phys.* **33** (1995) 129.
9. M. A. AFIFI, N. A. HEGAB and A. E. BEKHEET, *Vacuum* **47** (1996) 265.
10. S. R. OVSHINSKY, *Phys. Rev. Lett.* **21** (1968) 1450.
11. F. M. COLLINS, *J. Non-Cryst. Solids* **2** (1970) 496.
12. J. L. HARTKE, *Phys. Rev.* **125** (1962) 1177.
13. B. J. BAGLEY, *Solid State Commun.* **2** (1972) 4663.
14. D. EMIN, C. H. SEAGER and P. K. QUINN, *Phys. Rev. Lett.* **28** (1972) 813.
15. R. M. HILL, *Phil. Mag.* **23** (1972) 59.
16. M. A. AFIFI, N. A. HEGAB and A. E. BEKHEET, *Vacuum* **46** (1995) 335.
17. N. A. HEGAB, M. A. AFIFI, A. E. EL-SHAZLY and A. E. BEKHEET, *J. Mat. Science* **33** (1998) 2441.
18. J. T. KERR, *J. Non-Cryst. Solids* **2** (1970) 203.
19. W. SCHOTTKY, *Z. Physik* **15** (1914) 872.
20. J. FRENKEL, *Phys. Rev.* **54** (1938) 647.
21. D. N. BOSE and S. DE PURKAYASTHA, *Mat. Res. Bull.* **16** (1981) 635.
22. N. F. MOTT and E. A. DAVIS, "Electronic Processes in Non-crystalline Materials" (Clarendon, Oxford, 1971).
23. A. N. SREERAM, A. K. VARSHNEYA and D. R. SWILER, *J. Non-Cryst. Sol.* **130** (1991) 225.
24. A. R. HILTON, C. E. JONES and M. BARAU, *Phys. Chem. of Glasses* **7** (1966) 105.
25. I. WATANABE, S. KANEKO, H. KAWOZOE and M. YAMANE, *Phys. Rev. B* **40** (1989) 3133.
26. A. K. JONSCHER, *Thin Solid Films* **1** (1967) 213.

Received 14 April 1999

and accepted 7 February 2001